The Journal of Chemical Physics

Extension of frozen natural orbital approximation to open-shell references: Theory, implementation, and application to single-molecule magnets

Cite as: J. Chem. Phys. **152**, 034105 (2020); https://doi.org/10.1063/1.5138643
Submitted: 14 November 2019 . Accepted: 19 December 2019 . Published Online: 17 January 2020

Pavel Pokhilko, Daniil Izmodenov, and Anna I. Krylov

AIP Publishing

The Journal of Chemical Physics ARTICLE scitation.org/journal/jcp

Extension of frozen natural orbital approximation to open-shell references: Theory, implementation, and application to single-molecule magnets

Cite as: J. Chem. Phys. 152, 034105 (2020); doi: 10.1063/1.5138643
Submitted: 14 November 2019 • Accepted: 19 December 2019 •
Published Online: 17 January 2020

Pavel Pokhilko,[1] Daniil Izmodenov,[1,2] and Anna I. Krylov[1,a)]

AFFILIATIONS

[1]Department of Chemistry, University of Southern California, Los Angeles, California 90089-0482, USA
[2]Department of Chemistry, Lomonosov Moscow State University, Moscow 119991, Russia

[a)]Electronic mail: krylov@usc.edu

ABSTRACT

Natural orbitals are often used to achieve a more compact representation of correlated wave-functions. Using natural orbitals computed as eigenstates of the virtual–virtual block of the state density matrix instead of the canonical Hartree–Fock orbitals results in smaller errors when the same fraction of virtual space is frozen. This strategy, termed frozen natural orbital (FNO) approach, is effective in reducing the cost of regular coupled-cluster (CC) calculations and some multistate methods, such as EOM-IP-CC (equation-of-motion CC for ionization potentials). This contribution extends the FNO approach to the EOM-SF-CC ansatz (EOM-CC with spin-flip). In contrast to EOM-IP-CCSD, EOM-SF-CCSD relies on high-spin open-shell references. Using FNOs computed for an open-shell reference leads to an erratic behavior of the EOM-SF-CC energies and properties due to an inconsistent truncation of the α and β orbital spaces. A general solution to problems arising in the EOM-CC calculations utilizing open-shell references, termed OSFNO (open-shell FNO), is proposed. By means of singular value decomposition (SVD) of the overlap matrix of the α and β orbitals, the OSFNO algorithm identifies the corresponding orbitals and determines virtual orbitals corresponding to the singly occupied space. This is followed by SVD of the singlet part of the state density matrix in the remaining virtual orbital subspace. The so-computed FNOs preserve the spin purity of the open-shell orbital subspace to the extent allowed by the original reference, thus facilitating a safe truncation of the virtual space. The performance of OSFNO is benchmarked for selected diradicals and triradicals.

I. INTRODUCTION

The scope of applicability of correlated quantum chemical methods is limited by their steep scaling with respect to the system size.[1] To formulate the algorithms in terms of basic linear algebra operations, such as matrix multiplication, many-body wave-functions are represented by Slater determinants composed of molecular orbitals, which are, in turn, represented as an expansion over one-electron basis sets (i.e., atomic orbitals). Consequently, the ultimate scaling of a many-body method is determined not only by the number of electrons, but also by the number of basis functions. For example, the overall N^6 scaling of the coupled-cluster method with single and double excitations (CCSD) comes from the computational step involving O^2V^4 operations, where O and V denote the number of occupied and virtual orbitals, respectively.[2] Whereas the former is determined by the number of electrons, the latter depends on the number of basis functions. Explicit treatment of triple excitations, as in CCSDT,[3] leads to N^8 complexity, while perturbative treatments, such as in (T),[4–6] ($\tilde{\text{T}}$),[7] (2),[8] (dT),[9] (fT),[9] and related approaches,[10–12] give rise to N^7 scaling.

There are various strategies for reducing computational costs by using more compact representations of many-body

wave-functions and the Hamiltonian. The sparsity of two-electron repulsion integrals (ERI) can be utilized through the approximate representation using auxiliary basis sets obtained by density fitting, as in the resolution-of-identity (RI) methods,[13–21] or by the Cholesky decomposition of ERIs,[22–31] or using alternative schemes such as pseudospectral decomposition,[32–34] chain-of-spheres exchange,[35–37] and tensor hypercontraction.[38–42] Decomposition of amplitudes can also be used to reduce computational costs.[43–46] A number of strategies exploit the physical decay of Coulomb interaction with a distance by using localized orbitals.[47–50] Based on orbital localization and truncation of noninteracting orbital subsets, reduced-scaling versions of MP2,[51,52] CCSD,[53,54] (T) correction,[55–57] and beyond[58] have been developed.

More compact representations of correlated wave-functions can be achieved by using various flavors of natural orbitals (NOs), which has been exploited since early days of quantum chemistry. Natural orbitals, as introduced by Löwdin,[59] are defined as eigenvectors of a state one-particle density matrix:

$$\gamma_{pq} = \langle \Psi | p^\dagger q | \Psi \rangle, \tag{1}$$

where $p^\dagger/q$ denote creation and annihilation operators corresponding to spin orbitals ϕ_p/ϕ_q, and indices p, q run over all spin-orbitals. The trace of γ equals the number of electrons and its eigenvalues are non-negative numbers between 0 and 1. The magnitude of these eigenvalues, called occupation numbers, reflects the relative weights of configurations in which the respective NO is occupied. For example, for a single Slater determinant Φ composed of a subset of $\{\phi_p\}$, γ_{pq} is a diagonal matrix with $\gamma_{pp} = 1$ for the orbitals occupied in Φ and zero otherwise. Thus, molecular orbitals from a Hartree–Fock calculation are also natural orbitals of the underlying Hartree–Fock wave-function. Moreover, because all occupied orbitals have unit occupancy and all virtual orbitals have zero occupancy, any unitary transformation within the occupied or virtual space yields a set of Hartree–Fock natural orbitals. For multideterminantal wave-functions, the occupation numbers become fractional. Because the occupations are proportional to the relative weights of the configurations in which a particular orbital is occupied, one can use natural orbitals to compress the orbital space by dropping the orbitals with low occupation numbers. This utility of natural orbitals to compress correlated wave functions[59] has been exploited in a variety of configuration interaction methods.[60–68] More recently, hybrid approaches using both localization techniques and natural or pair-natural orbitals have led to the development of very effective computer implementations of modern many-body theories,[69–77] enabling, for example, CC calculations on a protein (crambin) consisting of more than 600 atoms and with more than 6000 basis functions.[73]

Here, we are concerned with a very simple strategy to reduce the computational cost of single-reference correlated calculations, that is, truncating the virtual orbital space while leaving the occupied space untouched, such that the exact correlation energy of a given method is smoothly recovered as the fraction of frozen virtual orbitals approaches zero. By using perturbation theory arguments, one can, of course, justify simply freezing high-lying canonical Hartree–Fock orbitals. However, natural occupations provide a much better gauge of the relative importance of orbitals in terms of their contributions into the total correlation energy. In order to preserve the definition of the vacuum (which is determined by choosing a particular reference determinant), the concept of Frozen Natural Orbitals (FNOs) was introduced.[78] FNOs are eigenstates of the virtual–virtual block of the one-particle density matrix; thus, they can be used to transform only the virtual space, without changing the reference determinant, as sketched in Fig. 1. Of course, to compute FNOs, one needs to know the full correlated wave-function. A typical strategy of using FNOs as a mean to reduce computational costs is to use a density matrix computed at a lower level of theory (say, MP2, which scales as N^5) to reduce the cost of higher-level calculations, such as CCSD or CCSD(T). This simple yet effective idea has been pioneered by Bartlett and coworkers[79–81] in the context of the ground-state CC calculations. The benchmarks have shown that significant computational gains can be achieved while introducing insignificant errors in the optimized geometries, relative energies, barrier heights,[80,81] as well as in noncovalent interactions.[82] However, calculations of response properties have proven to be more challenging, requiring modification of the approach.[83,84]

By definition, natural orbitals are state-specific, reflecting the state-specific nature of correlation. Consequently, exploiting natural orbitals within multistate calculations is not straightforward. The difficulty of applying natural orbitals to excited states stems from the fact that a one-size-fits-all truncation of the orbital space is likely to introduce an imbalance in the excited-states description. One can even imagine an extreme situation when the truncation based on correlation for one state would exclude the orbitals that are needed to describe the principal character of another state. For example, choosing orbitals based on their contributions to the ground-state correlation energy is likely to provide a reasonable virtual space for low-lying valence states (e.g., HOMO-LUMO excitations); however, it would exclude orbitals needed for the description of Rydberg states because diffuse orbitals are not very important for ground-state correlation. Nevertheless, several ideas have been explored in the context of single-reference excited-state calculations, including using state-specific or averaged NOs,[85] pair natural orbitals,[86] and natural transition orbitals.[87,88]

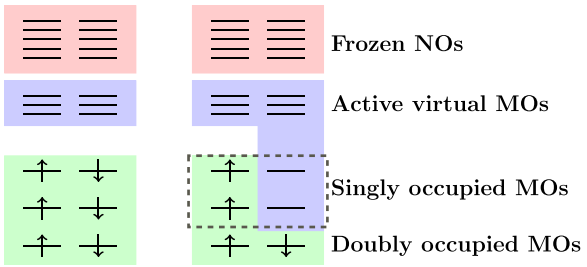

FIG. 1. Frozen natural orbitals (FNOs) are defined as eigenstates of the virtual-virtual block of a correlated state density matrix. In the FNO approach, the occupied space is unchanged, but the virtual orbital space is transformed such that the orbitals can be ordered by their relative significance for the correction energy and the orbitals with the lowest occupations can be frozen. Left and right panels highlight the difference between calculations using closed- and open-shell references. Because in the latter the α and β orbital spaces are different, a special care is needed to arrange the orbitals by maximum correspondence, so that dropped orbitals do not introduce an imbalance in the singly occupied space (marked by dashed box).

In contrast to general excited-state calculations, virtual space truncation schemes based on a single-state density matrix are admissible in selected multistate Fock-space methods, such as equation-of-motion coupled-cluster (EOM-CC); see Fig. 2.[89–92] For example, multiple ionized states can be described in a balanced way by using a virtual space truncation scheme based on the density matrix computed for the closed-shell reference state[93] because the principal character of ionized (i.e., *hole*) states is confined to the occupied orbital space. This idea,[93] originally explored within FNOs,[93] has been recently extended to the domain local pair-natural orbitals.[77] Here, we extend the idea of using reference-state FNOs to other EOM-CC methods.

The EOM-CC family of methods[89–92] is based on the Fock-space parameterization of the wave-function. EOM-CC is a multistate approach in which different manifolds of target states are described by choosing a particular combination of a reference state and a general excitation operator. General excitation operators in single-reference theories are defined with respect to the reference state, which defines the separation of the occupied and virtual orbital spaces; they can include only creation (i.e., particle) operators corresponding to the virtual orbitals and annihilation (i.e., hole) operators corresponding to the occupied orbitals. The reference state is described by the CC ansatz, which incorporates large amount of correlation and endows the theory with such important property as size-extensivity. Different flavors of EOM-CC are illustrated in Fig. 2. Electronically excited states are described by particle- and spin-conserving excitations from (usually) a closed-shell reference corresponding to the ground state, giving rise to the EOM-EE-CC method. Cationic or neutral doublet states can be described by ionizing operators such as 1-hole (1*h*) and 2-hole-1-particle (2*h*1*p*) acting on a closed-shell reference, giving rise to EOM-IP.[94,95] Doubly ionizing operators (2*h* and 3*h*1*p*) can be used to access diradical-type or doubly ionized states (EOM-DIP). In a similar fashion, electron attaching operators (1*p*, 1*h*2*p*) acting on a closed-shell reference provide access to anionic or neutral doublet states (EOM-EA).[96] Double electron attaching operators (2*p* and 3*p*1*h*) provide access to diradical states or to a subset of excited states derived from excitation from HOMO (EOM-DEA). By using high-spin references and spin-flipping operators,[97–99] other types of multiconfigurational states can be described (EOM-SF and EOM-DSF).

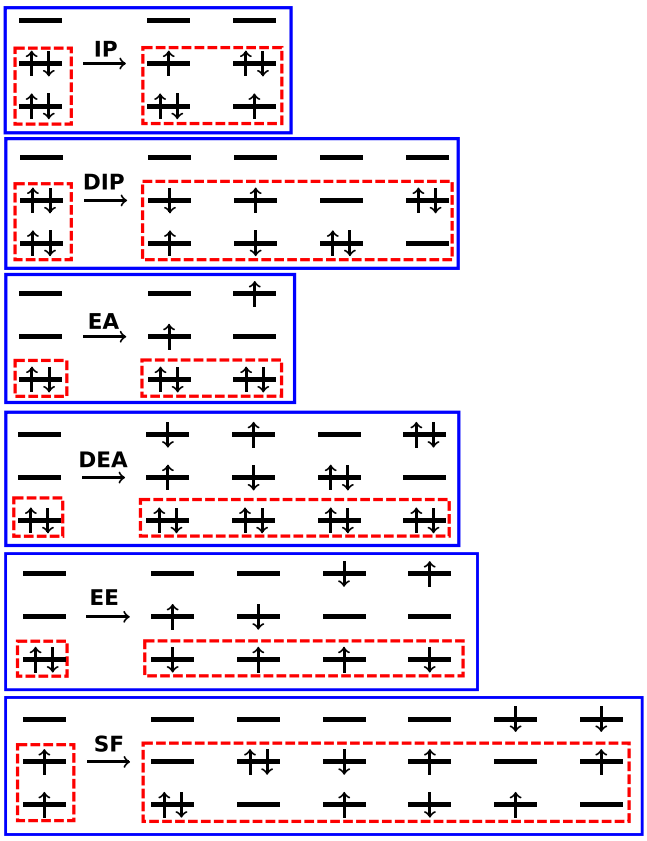

FIG. 2. In the EOM-CC formalism, different manifolds of target states are described by combining a particular reference state and a particular type of excitation operator (orbitals occupied in the reference state are marked by red dashed boxes). Note that in EOM-IP and EOM-DIP, the principal character of target states is described by the hole operators acting in the occupied orbital space (red boxes), whereas in EOM-EA and EOM-DEA it is described by the particle operators acting in the virtual space. In EOM-EE, the EOM operators act in both spaces. In EOM-SF (spin-flip), the leading electronic configurations of the target states are confined to the singly occupied orbital space.

Figure 2 clearly distinguishes between three groups of EOM-CC methods: one in which the principal character of target states is described by annihilation operators (EOM-IP and EOM-DIP), one in which the principal character is described by creation operators (EOM-EA and EOM-DEA), and one in which the principal character is described by both creation and annihilation operators (EOM-EE, EOM-SF, and EOM-DSF). For the first group of methods, FNOs derived from the reference state density matrix should provide a reasonable recipe for the virtual space truncation, since the virtual space is primarily responsible for describing correlation of the target states. However, for the second group, truncation of the virtual space affects the description of the leading configurations of the target states, thus suggesting that the FNOs derived from the reference-state density matrix may not provide an optimal and balanced truncation scheme. The methods from the third group present an interesting case. Whereas, the quality of the EOM-EE states can be adversely affected by the virtual space truncation based on the ground-state correlation (as in the hypothetical example of Rydberg and valence states discussed above), the quality of the EOM-SF states should not be compromised by the virtual space truncation based on the reference-state correlation because the virtual orbitals needed to describe the target spin-flip states should have the same character as the occupied orbitals hosting the unpaired electrons in the high-spin reference. In other words, because the singly occupied orbital space (see Fig. 1) is well defined by the choice of the high-spin reference, one can develop an effective truncation scheme of the rest of the virtual space based on the FNOs defined by the reference-state density matrix. Here, we develop this idea into a practical algorithm of virtual space truncation by using the singular value decomposition (SVD) procedure and illustrate the performance of the resulting method by calculations of multiple electronic states and interstate properties in selected diradicals and triradicals. We note that although EOM-SF-CC is a single-reference method and does not employ active spaces, the singly occupied orbital space defined by

our procedure is conceptually similar to an active space of strongly correlated orbitals used within multireference formalisms.[67,100,101] The utility of natural orbitals computed for high-spin states in multireference calculations of ground and low-lying excited states has been successfully exploited[67,68] by Lu and Matsika.

II. THEORY

A. Equation-of-motion coupled-cluster methods

The wave-function in the EOM-CC methods is parameterized as

$$|\Psi_I\rangle = \hat{R}_I e^{\hat{T}}|\Phi_0\rangle, \tag{2}$$

where $\hat{T}$ is a coupled-cluster excitation operator, Φ_0 is a reference determinant, and $\hat{R}$ is an excitation[102] (EOM-EE-CCSD), spin-flip[97–99] (EOM-SF-CCSD and EOM-DSF-CCSD), ionization[94,95] (EOM-IP-CCSD and EOM-DIP-CCSD), or electron-attachment[96] (EOM-EA-CCSD and EOM-DEA-CCSD) operator. EOM amplitudes R are obtained by diagonalization of the similarity-transformed Hamiltonian $\bar{H}$ on the basis of the determinants from the corresponding sector of the Fock space as follows:

$$\bar{H} = e^{-T} H e^{T}, \tag{3}$$

$$\bar{H} R_I = E_I R_I, \tag{4}$$

$$L_I \bar{H} = L_I E_I. \tag{5}$$

Because $\bar{H}$ is non-Hermitian, it has distinct right and left eigenvectors, which can be chosen to form a biorthogonal set as follows:

$$L_I R_J = \delta_{IJ}. \tag{6}$$

Once the left and right eigenstates of $\bar{H}$ are computed, properties are evaluated as contraction of the corresponding integrals with appropriate density matrices. Evaluation of the expectation value of a one-electron operator $\hat{A}$ requires one-electron density matrix γ,

$$\hat{A} = \sum_{pq} \langle \phi_p | A | \phi_q \rangle p^\dagger q, \tag{7}$$

$$\langle \Psi_I | \hat{A} | \Psi_J \rangle = \sum_{pq} \langle \phi_p | A | \phi_q \rangle \langle \Psi_I | p^\dagger q | \Psi_J \rangle = \sum_{pq} \langle \phi_p | A | \phi_q \rangle \gamma_{pq}^{I \to J}, \tag{8}$$

where the labels I and J enumerate electronic states. Because of the non-Hermitian nature of EOM-CC, $I \to J$ and $J \to I$ transition densities are different, resulting in different numerical values of the A_{IJ} and A_{JI} matrix elements. Geometric[102] or arithmetic average[103–105] of the matrix elements can be used to handle this discrepancy.

When $\hat{R}$ includes all possible excitations, EOM-CC is equivalent to full configuration interaction (FCI). Practical approximate methods are based on truncation of $\hat{R}$ (and $\hat{T}$) at some excitation level, i.e., in EOM-SF-CCSD, $\hat{R}$ is truncated at single and double excitations,

$$R^{SF} = \sum_{ia} r_i^a a^\dagger i + \frac{1}{4} \sum_{ijab} r_{ij}^{ab} a^\dagger b^\dagger j i, \tag{9}$$

where i and a denote occupied and virtual (with respect to Φ_0) spin-orbitals. $\hat{T}$ is usually truncated at the same excitation level and has the same general form as Eq. (9), except that $\hat{T}$ is an $M_S = 0$ operator (i.e., only the $\alpha\alpha$ and $\beta\beta$ blocks are nonzero in T_1), whereas R^{SF} is an $M_S = -1$ operator (only the $\alpha\beta$ block is nonzero in R_1^{SF}). The truncation at the level of double excitations results in the N^6 scaling of the method. The approximations used within the EOM-CC framework preserve a number of important properties, such as orbital invariance with respect to the rotations in the occupied or virtual spaces and size consistency (or size-intesivity). The accuracy of EOM-SF can be systematically improved (up to the FCI limit) by including higher excitations. The benchmarks illustrate that even the lowest-level of EOM-SF methods yield accurate energy gaps due to the built-in balanced treatment of multiple electronic states. For example, when applied for calculating singlet and triplet states in diradicals, EOM-SF-CCSD provides excitation energies with the error bar of 0.03–0.05 eV;[9,106] the benchmark study on dicopper single-molecule magnets (SMMs)[107] have shown that even very small energy gaps of several hundreds or tens of wave numbers can be resolved.

B. FNO algorithm for closed- and open-shell references

The original closed-shell FNO approximation is defined by the following algorithm:[93]

1. Start from canonicalized orbitals.
2. Compute MP2 T_2 amplitudes.
3. Compute the VV part of the MP2 density matrix for the reference state, γ^{vv}.
4. Diagonalize γ^{vv} to obtain NOs, sort them according to their occupation numbers in the descending order.
5. Freeze the NOs with the lowest occupation numbers according to a given criterion (either a fixed fraction of the virtual space or a fraction of the virtual space needed to recover the specified population threshold[93]).
6. Semicanonicalize active orbitals (this step is optional; it is recommended for faster convergence of iterative eigensolvers).
7. Carry out the transformation of the required integral blocks into the new orbital basis (only the blocks involving virtual orbitals need to be transformed).
8. Execute CCSD, CCSD(T), EOM-IP-CCSD, EOM-DIP-CCSD, etc. in the truncated orbital space.

As illustrated below by numerical examples, the application of this procedure to an open-shell reference results in an erratic behavior, attributed to an unbalanced truncation of the α and β virtual orbital spaces. To solve this problem, we developed an algorithm for separating the virtual β space into a subspace matching the orbitals which are singly occupied in the high-spin reference and the rest. This procedure (which we named OSFNO) effectively determines the singly occupied subspace and uses the same strategy as proposed in Ref. 108. We note that the issue of unbalanced truncation of α and β spaces does not appear in fully spin-adapted formulations, such as the one used by Lu and Matsika.[67,68]

The correspondence between two sets of orbitals can be established by means of SVD of the overlap matrix: singular values of one

reveal the orbitals matching exactly, whereas smaller values correspond to partial overlap and zeros correspond to orthogonal subspaces. Thus, SVD of the overlap between the α occupied and β virtual orbitals allows us to identify the orbitals from the singly occupied subspace. In all considered systems, two (for triplet references) or three (for quartet references) singular values of the overlap matrix are very close to one, clearly identifying the open-shell electrons, while all other singular values are much smaller.

Assuming that the reference is a high-spin state in which the number of α electrons is larger than the number of β electrons, the OSFNO algorithm proceeds as follows:

1. Compute the overlap matrix between the occupied α and virtual β orbitals: $S_{ov}^{\alpha\beta} = (C_{\alpha,o}^{MO})^{\dagger} S^{AO} C_{\beta,v}^{MO}$.
2. Perform SVD of the overlap matrix: $S_{ov}^{\alpha\beta} = U_{\alpha}^{SVD} \Sigma (V_{\beta}^{SVD})^{\dagger}$.
3. Save singular vectors U^{SVD} and V^{SVD}.
4. Compute new C-matrices:
   $C_{\alpha,o}^{SVD\text{-}MO} = C_{\alpha,o}^{MO} U_{\alpha}^{SVD}$,
   $C_{\beta,v}^{SVD\text{-}MO} = C_{\beta,v}^{MO} V_{\beta}^{SVD}$.
5. Using near-unity singular values as a guide, eliminate open-shell subspace v and β to form a virtual subspace $\tilde{v}$ from which the open-shell orbitals are excluded.
6. Compute MP2 T_2 amplitudes in the basis of the original MOs.
7. Compute the VV part of the MP2 state density matrix γ^{vv} in the basis of the original MOs.
8. Carry out MO → AO transformation (without multiplication by S^{-1}) of γ^{vv}, make $\gamma_{\alpha\alpha}^{AO}$ and $\gamma_{\beta\beta}^{AO}$.
9. Extract the singlet density $\gamma^{AO,S} = \frac{1}{\sqrt{2}}\left(\gamma_{\alpha\alpha}^{AO} + \gamma_{\beta\beta}^{AO}\right)$.
10. Transform $\gamma^{AO,S}$ to the new $\alpha\beta$ $\tilde{v}$ orbitals:
$$\gamma_{\alpha\beta}^{\tilde{v}\tilde{v},S} = C_{\alpha,\tilde{v}}^{\dagger} S^{AO} \gamma^{AO,S} S^{AO} C_{\beta,\tilde{v}}.$$
11. Perform SVD of $\gamma_{\alpha\beta}^{\tilde{v}\tilde{v},S}$.
12. Sort density singular values, freeze $\alpha\beta$ pairs according to a given criterion (the criteria are the same as in the original FNO scheme[93]).
13. Semicanonicalize the active orbitals (optional).
14. Transform the required integral blocks to the new orbital basis.
15. Carry out CCSD and EOM-SF-CCSD in the truncated orbital space.

Steps 1–5 separate the open-shell space from the rest of the orbitals. The singlet part of the density is taken because it has the same $\alpha\alpha$ and $\beta\beta$ parts and it is consistent with the closed-shell case. The correspondence between the α and β NOs is established through SVD of the density matrix between the α and β orbitals. The selection criterion for the $\alpha\beta$ pairs is the respective singular values. We implemented this algorithm in the Q-Chem electronic structure package.[109,110]

C. Computational details

We investigated the performance of the FNO approximation within the EOM-SF-CCSD method for the set of prototypical diradicals and triradicals:

1. Methylene (CH_2) and isolectronic species: NH_2^+, SiH_2, and PH_2^+. We used geometries of the $^3B_1$ states from Ref. 111. Dunning's cc-pVTZ basis set was used.

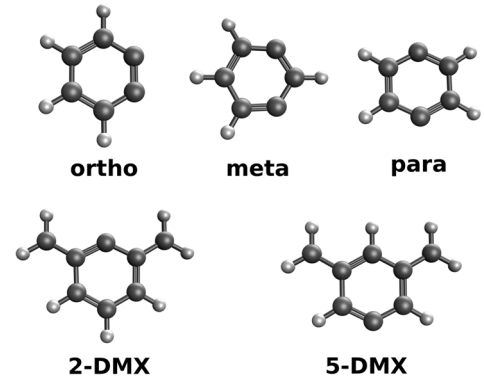

FIG. 3. Structures of benzynes and dehydro-*meta*-xylylenes.

2. Benzynes: *ortho*-, *meta*-, and *para*-benzynes (Fig. 3). We used geometries of the $^3B_2$ states from Ref. 111 (optimized with NC-SF-TDDFT/LDA/cc-pVTZ). We used the cc-pVTZ basis set.
3. 2- and 5-dehydro-*meta*-xylylene (DMX) triradicals (Fig. 3). The geometries were optimized with the CCSD/cc-pVDZ for the quartet states and are given in the supplementary material. Single-point EOM-SF-CCSD calculations were performed with the cc-pVTZ basis set.
4. Two-center copper SMMs: PATFIA (without ferrocene group, see Fig. 4), CITLAT, and BISDOW. The geometries (optimized with ωB97X-D/cc-pVTZ for the triplet state) were taken from Ref. 107. Triplet's ωB97X-D/cc-pVTZ geometry of CUAQAC02 is given in the supplementary material. The EOM-SF-CCSD calculations of SMMs were carried out using single precision for CCSD, the intermediates, and EOM amplitudes,[112] and with the Cholesky decomposition of ERIs[29] (threshold of 10^{-2}). Most of the EOM-SF-CCSD calculations were performed with the cc-pVDZ basis set; for PATFIA, one single point calculation was also evaluated with the cc-pVTZ basis set.

The reported symmetry labels of the electronic states and MOs correspond to Mulliken's convention.[113,114]

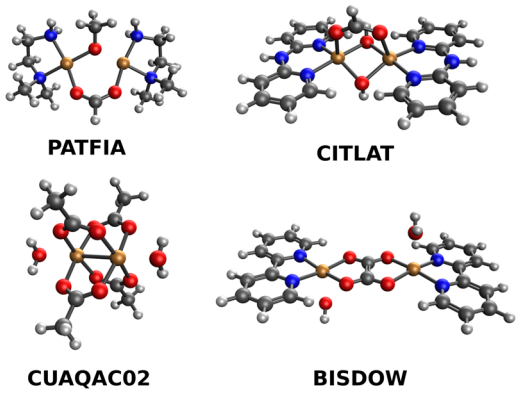

FIG. 4. Structures of SMMs. Color scheme: Bronze (copper), blue (nitrogen), red (oxygen), gray (carbon), and white (hydrogen).

TABLE I. Vertical excitation energies relative to the $^3B_1$ state in the methylene series computed with EOM-SF-CCSD/cc-pVTZ in the full virtual space at the triplet state geometry. UHF and ROHF references were used.

	UHF			ROHF		
Systems	$\tilde{b}^1B_1$	$\tilde{a}^1A_1$	$\tilde{c}^1A_1$	$\tilde{b}^1B_1$	$\tilde{a}^1A_1$	$\tilde{c}^1A_1$
CH_2	1.52	0.94	3.29	1.52	0.94	3.29
NH_2^+	1.94	1.82	3.57	1.94	1.82	3.57
SiH_2	1.13	−0.42	3.40	1.13	−0.42	3.40
PH_2^+	1.27	−0.17	3.72	1.27	−0.18	3.72

To compare the compactness of virtual spaces obtained with the FNO and OSFNO schemes with the results of spin-adapted FNO-CISD calculations by Lu and Matsika,[67] we considered the lowest triplet state of formaldehyde at the ground-state CCSD/cc-pVDZ geometry; the Cartesian coordinates are given in the supplementary material.

Core electrons were frozen in correlated calculations. All calculations were carried out with the Q-Chem package.[109,110]

III. RESULTS AND DISCUSSION

Tables I–III summarize relevant energy gaps computed with EOM-SF-CCSD/cc-pVXZ for the diradicals and triradicals used as a benchmark in this work. The structures of the molecules are shown in Figs. 3 and 4. Detailed discussion of their underlying electronic structure can be found in Refs. 106, 115, 116, and 107. The singlet–triplet gaps in copper diradicals are given in Table III. For the methylene series, we consider the manifold of all 4 diradical states (2 closed-shell singlets, open-shell singlet, and triplet), whereas for the rest of the systems we focus on the two lowest states and consider only the singlet-triplet and doublet-quartet gaps.

A. Analysis of the original FNO approximation and comparison with OSFNO

As the first example, we consider the methylene diradical. Direct application of the original FNO scheme to the CCSD calculation of the high-spin triplet state yields errors of a similar magnitude as in the closed-shell FNO calculations,[93] as illustrated in Fig. S2 in the supplementary material. However, errors in the EOM-SF-CCSD energies are considerably larger, as shown in Fig. 5. Already at a small truncation of the total population (a few percent), the errors reach a magnitude of one electron-volt. Such a rapid growth of the errors can be explained in terms of contributions of the physically important orbitals responsible for strong correlation (i.e., those from the singly occupied subspace) to the frozen virtual orbital space. The singlet–triplet gap between the two lowest EOM states also shows large errors (Fig. S3). The origin of the problematic behavior is revealed by the $\langle S^2 \rangle$ calculations: as shown in the top panel of Fig. 6, the trends in spin contamination of the open-shell states follow each other in a symmetric manner, suggesting that these two states are mixed. We rationalize this trend in $\langle S^2 \rangle$ by considering the following model for open-shell states:

$$\Psi_T = \frac{1}{\sqrt{1+\lambda^2}}\left(\Psi_T^\circ + \lambda \Psi_S^\circ\right), \tag{10}$$

$$\langle \Psi_T | S^2 | \Psi_T \rangle = \frac{2}{1+\lambda^2}, \tag{11}$$

where T and S denote the triplet and the singlet, respectively. Let us denote the states computed with the full virtual orbital space as Ψ_T° and Ψ_S° and the states computed with the truncated virtual

TABLE II. Vertical singlet–triplet and doublet–quartet gaps (eV) computed with EOM-SF-CCSD/cc-pVTZ in the full virtual space at the triplet/quartet state geometry (negative sign corresponds to the singlet/doublet ground states) using UHF and unrestricted Kohn-Sham DFT/PBE reference orbitals.

Reference	S	T	*o*-C_6H_3	*m*-C_6H_3	*p*-C_6H_3[a]
UHF	$^1A_1$	$^3B_2$	−0.99	−0.51	−0.14
PBE	$^1A_1$	$^3B_2$	−1.00	−0.52	−0.14
Reference	D	Q	2-DMX	5-DMX	
UHF	$^2B_2$	$^4B_2$	0.45	−0.53	
PBE	$^2B_2$	$^4B_2$	0.42	−0.20	

[a]For *para*-benzyne the symmetries of electronic states in the full point-group symmetry are ^1A_g and $^3B_{1u}$.

TABLE III. Singlet–triplet gaps in SMMs (cm^{-1}) computed with UHF EOM-SF-CCSD/cc-pVDZ in full virtual spaces (negative sign corresponds to the singlet ground state).

Molecule	ΔE
PATFIA	−85
CITLAT	121
CUAQAC02	−191
BISDOW	−225

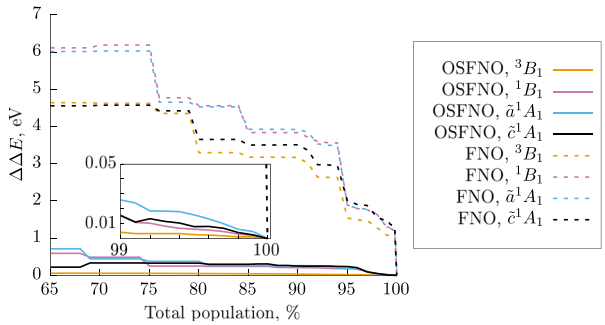

FIG. 5. Errors in energy differences ($\Delta\Delta E$, eV) between the four EOM-SF-CCSD target states (M_S = 0 triplet component, open-shell singlet, and two closed-shell singlets) and the reference high-spin triplet CCSD state of CH_2 computed with cc-pVTZ. Two schemes are shown: the original FNO (dashed lines) and the new open-shell variant (solid lines). The errors are computed relative to the full spaces EOM-SF-CCSD values.

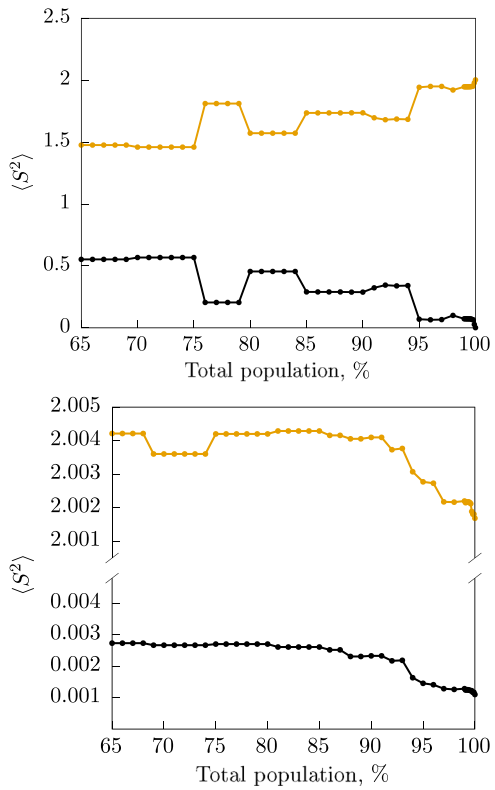

FIG. 6. $\langle S^2 \rangle$ for open-shell singlet and triplet states of CH_2 obtained by the original FNO approximation (top) and OSFNO (bottom); EOM-SF-CCSD/cc-pVTZ.

space as Ψ_T and Ψ_S. The mixing parameter λ connects $\langle S^2 \rangle$ and the occupancies of frontier natural orbitals,

$$n_\alpha - n_\beta = \frac{2\lambda}{1+\lambda^2}, \tag{12}$$

$$(n_\alpha - n_\beta)^2 = -\langle \Psi_T | S^2 | \Psi_T \rangle^2 + 2\langle \Psi_T | S^2 | \Psi_T \rangle, \tag{13}$$

where n_α and n_β are the occupancies of the corresponding α and β frontier natural orbitals of the triplet state. For spin-pure open-shell states with zero spin projection, $n_\alpha = n_\beta$. Figure 7 shows $(n_\alpha - n_\beta)^2$ vs

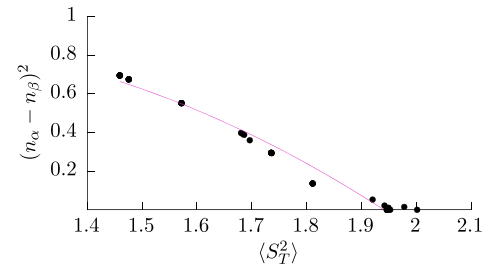

FIG. 7. Analysis of the imbalance between the α and β orbital spaces in the FNO EOM-SF-CCSD/cc-pVTZ calculation of the $M_s = 0$ triplet state of CH_2, see the text and Eq. (13).

$\langle S^2 \rangle$, both computed for the EOM-SF-CCSD wave-functions of CH_2 as a function of the FNO threshold. A close correlation between the two quantities confirms that the above model of state mixing indeed captures the essence of the problem.

Because the $\alpha\alpha$ and $\beta\beta$ blocks of the density matrix were diagonalized separately, there is no guarantee of direct correspondence between the α and β NOs. Moreover, the numerical values of the α and β occupancies are different. Sometimes, the α and β orbitals are ordered in a different manner. This introduces an imbalance between the frozen α and β orbital subspaces, causing spin contamination.

As described in Section II B, the OSFNO algorithm allows one to identify the open-shell orbitals and to match the virtual natural orbitals in a consistent manner, without introducing an imbalance between the α and β orbital spaces. Consequently, the spin contamination of the resulting states is minimal, as illustrated in the bottom panel of Fig. 6. The errors in energy gaps are also greatly reduced (Fig. 5).

We observe consistent robust performance of OSFNO for all test cases. We note that the orbital space truncation is far less detrimental to the CCSD energies than to the EOM-CCSD ones: the errors in FNO-CCSD relative to the full-space CCSD are always small and behave smoothly with respect to the truncation threshold. This observation is consistent with small errors reported by Neese and co-workers[76] for their DLPNO scheme. Consequently, OSFNO and FNO results for the high-spin triplet reference states are very similar for all considered systems, as shown in Fig. S2 in the supplementary material. For the target EOM-SF states, OSFNO leads to consistent improvement over the original FNO scheme: the position of the EOM-SF-CCSD states relative to the reference as well as the energy gaps between the target EOM states are improved dramatically (Fig. 5, S1, and S3).

Figure 8 compares errors in energy differences between the four EOM-SF-CCSD target states computed with the same number of frozen virtual orbitals using the OSFNO scheme and canonical

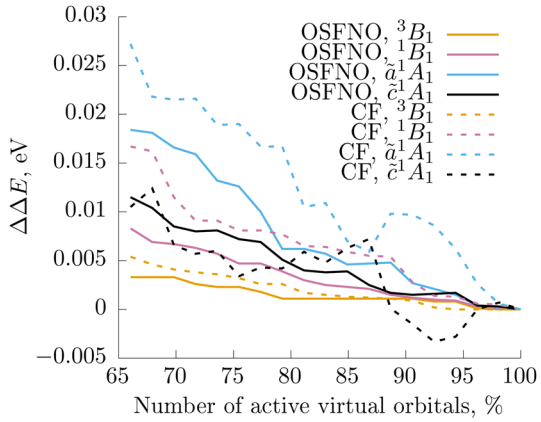

FIG. 8. Errors in energy differences ($\Delta\Delta E$, eV) between the four EOM-SF-CCSD target states ($M_S = 0$ triplet component, open-shell singlet, and two closed-shell singlets) and the reference high-spin triplet CCSD state of CH_2 computed with cc-pVTZ. Two schemes are compared: OSFNO and freezing the same fraction of canonical orbitals (canonical freezing, CF).

Hartree–Fock orbitals. Just as in the closed-shell case,[93] OSFNO performs better than freezing the same number of the canonical orbitals. Interestingly, freezing canonical orbitals leads to erratic behavior when very small number of orbitals is frozen (~10%), likely also because of the mismatch between the canonical α and β virtual spaces.

Overall, for the methylene-like diradicals, mean errors of OSFNO for a typical total population of 99% are 0.02–0.03 eV (130 cm^{-1} for an open-shell singlet-triplet gap, 200 cm^{-1} for a gap between closed-shell singlet and the triplet states).

B. Benzynes

An excellent performance of the SF methods in calculations of singlet–triplet gaps in benzynes and similar aromatic diradicals and triradicals has been illustrated in several benchmark studies.[9,106,116–121] An important prerequisite for accuracy is using not too spin-contaminated reference. In the case of large spin contamination of the UHF reference, ROHF orbitals, orbitals optimized for a correlated ansatz (i.e., approximate Brueckner's orbitals[122]), such as OO-CCD[123] or OO-MP2,[124,125] or even Kohn-Sham DFT orbitals[126–128] can be used. As shown below, the spin contamination of the reference state also affects the performance of the OSFNO approximation.

In the *ortho* → *meta* → *para*-benzyne series, the computed singlet–triplet energy gaps (−0.99, −0.51, and −0.14 eV) reflect an increased diradical character. In calculations with the UHF orbitals, we observe the largest error due to OSFNO in the singlet–triplet gap for the *meta* isomer, up to 200 cm^{-1} at 99% of the total unfrozen population (Fig. 9, UHF). The large errors for *meta*-benzyne can be attributed to the significant spin contamination of the reference determinant. To mitigate the effect of spin contamination, we explored using the ROHF orbitals, Kohn-Sham DFT/PBE orbitals, and OO-MP2 orbitals (computed with the RI approximation for the MP2 part).

Table IV compares the degree of spin contamination with different orbital choices. For benzynes, PBE and OO-MP2 provide a comparable reduction of spin contamination of the reference determinant, reducing the error in the singlet–triplet gap at 99% of total population to 54 and 60 cm^{-1}, respectively. The errors in singlet–triplet gaps with the ROHF orbitals for *meta*- and *para*-isomers are similar to those with the PBE and OO-MP2 orbitals: 66 and 8 cm^{-1}, respectively. We could not converge a ROHF calculation for *ortho*-benzyne.

C. Triradicals

To investigate the applicability of the OSFNO algorithm beyond diradicals, we considered two isomers of the dehydro-*meta*-xylylene (DMX) triradicals[117,129], 2- and 5-DMX. Previous studies[117,129] have shown that the ground state of 2-DMX is quartet $^4B_2$ and the ground state of 5-DMX is doublet $^2B_2$. The computed doublet–quartet energy gaps are: 0.45 and −0.53 eV for 2-DMX and 5-DMX, respectively. Figure 10 shows the errors in doublet–quartet gaps in 2- and 5-DMX. As in the case of benzynes, the UHF reference determinant of DMX is significantly spin-contaminated: $\langle S^2 \rangle$ is 4.45 for 2-DMX and 4.29 for 5-DMX. The spin contamination of the reference determinant is eliminated almost entirely using the PBE

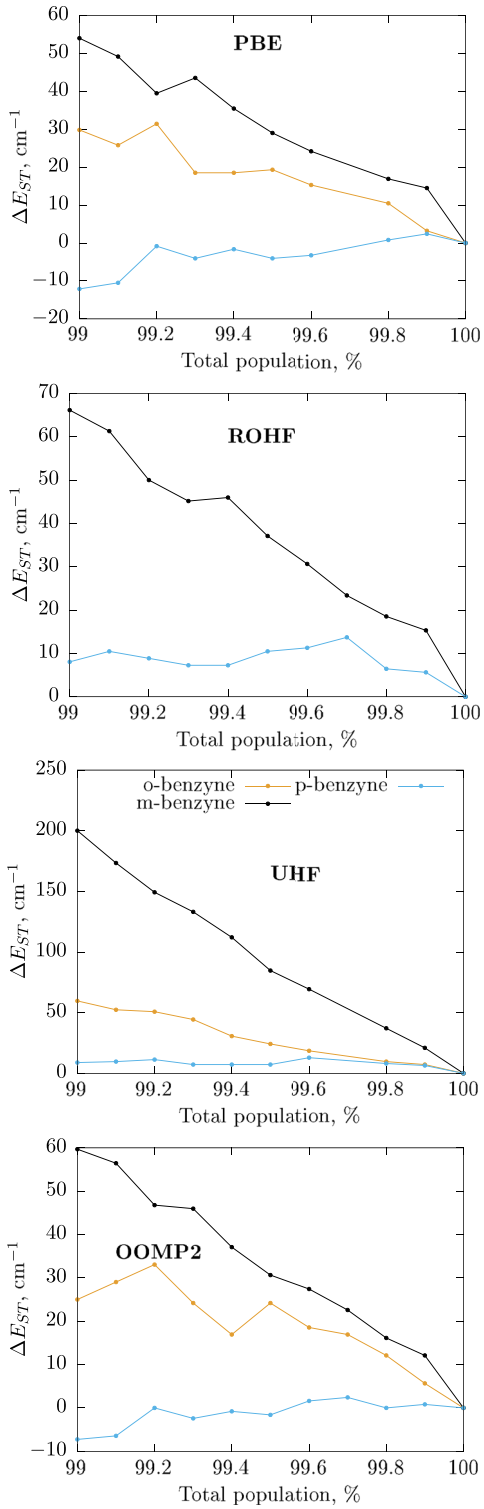

FIG. 9. Errors in singlet–triplet energy gaps for *ortho*-, *meta*-, and *para*-benzynes computed with EOM-SF-CCSD/cc-pVTZ and different orbitals (ROHF, UHF, PBE, and OO-MP2).

TABLE IV. $\langle S^2 \rangle$ values of the reference determinant for different orbital choices in benzynes; the cc-pVTZ basis set.

Isomer	UHF	PBE	OO-MP2
Ortho	2.206	2.007	2.011
Meta	2.681	2.015	2.025
Para	2.022	2.007	2.010

orbitals, which also significantly reduces the errors of OSFNO for doublet–quartet gaps.

D. Dicopper SMMs

The lowest singlet and triplet states in the dicopper SMMs have nearly perfect diradical character.[107,116] The interaction between the two radical centers is rather weak, owing to the large spatial separation between them and a relatively compact size of the *d*-orbitals. Consequently, the dynamic correlation in the singlet and triplet states is very similar, leading to rather small errors in the OSFNO calculations of the singlet–triplet gaps not exceeding 18 cm^{-1} (Fig. 11). Encouraged by small errors introduced by OSFNO, we carried out the EOM-SF-CCSD calculation for PATFIA with cc-pVTZ (1038 orbitals in total). Using the threshold, 99% of total population corresponds to freezing 429 virtual orbitals. The resulting exchange constant differs by less than 1 cm^{-1} from the cc-pVDZ result, thus validating the computational protocol used in Ref. 107.

E. Properties

To benchmark OSFNO beyond energy gaps, we computed spin–orbit coupling constants (SOCC) in the methylene series between the triplet and closed-shell EOM-SF states within mean-field spin-orbit approximation using the algorithm described in Ref. 105. The results are collected in Table V and shown graphicaly in Fig. 12. In all cases, we observed that the errors in SOCC due to OSFNO are less than 2.5 cm^{-1}, which is comparable with the accuracy of the mean-field approximation. The good performance of OSFNO for properties indicates that the truncation does not compromise the quality of the wave-functions.

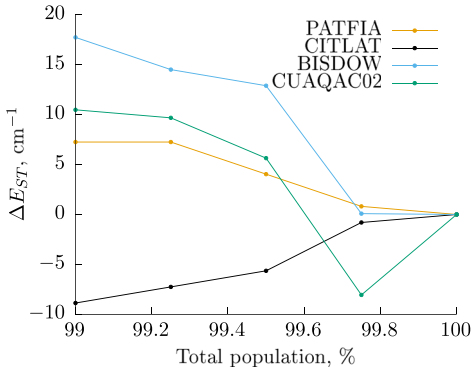

FIG. 11. Errors in the singlet–triplet gaps in selected SMMs calculated with cc-pVDZ.

TABLE V. Spin–orbit coupling constants (cm^{-1}) in selected diradicals, computed with EOM-SF-CCSD/cc-pVTZ in the full virtual orbital space. Couplings of the triplet and two states of closed-shell character are shown.

System	$^3B_1/\tilde{a}^1A_1$	$^3B_1/\tilde{c}^1A_1$
CH_2	10.9	20.7
SiH_2	56.7	86.0
NH_2^+	18.3	68.4
PH_2^+	119.9	175.6

F. Compactness of the OSFNO truncated virtual space

We conclude by comparing the compactness of the truncated virtual space obtained with the OSFNO and FNO schemes. Table VI shows the number of frozen orbitals in the calculation of the lowest triplet state of formaldehyde for the population threshold of 99%. The OSFNO leads to smaller numbers of frozen orbitals than FNO.

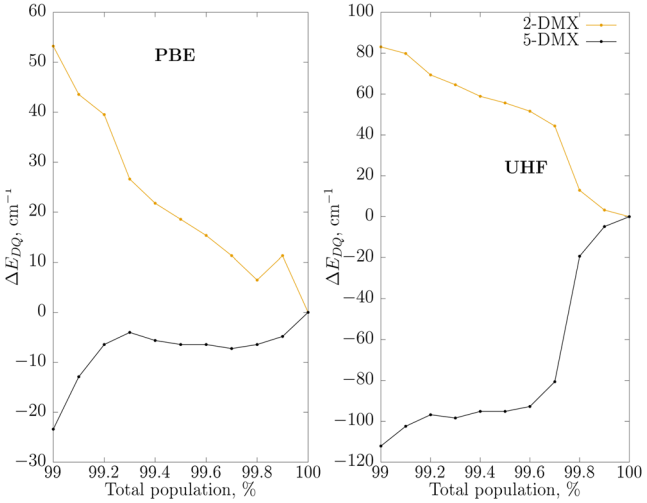

FIG. 10. Errors in doublet–quartet gaps in the two DMX triradicals computed with cc-pVTZ.

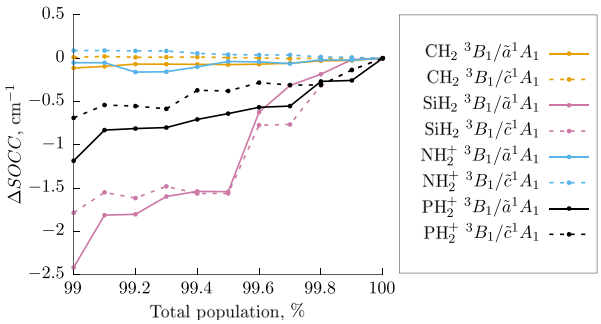

FIG. 12. Errors in spin–orbit coupling constant for transitions between triplet and two closed-shell singlet states of XH_2, EOM-SF-CCSD/cc-pVTZ.

TABLE VI. The number of frozen orbitals in different FNO approaches for the lowest triplet state of formaldehyde. The same freezing criterion was applied: occupation truncation threshold preserving 99% of virtual space population.

Basis	FNO-CISD[a]	FNO	OSFNO
cc-pVDZ	4	6	5
cc-pVTZ	30	32	30
cc-pVQZ	97	96	92

[a]From Ref. 67.

However, the differences between the two schemes are very small and the overall compactness of the resulting active virtual spaces is similar. We also compare our results with the FNO-CISD results of Lu and Matsika obtained within the spin-adapted framework and observe similar behavior.

IV. CONCLUSION

Using natural orbitals computed as the eigenstates of the virtual–virtual block of the state density matrix instead of the canonical Hartree–Fock molecular orbitals results in smaller errors when the same fraction of virtual orbitals is frozen.[93] Moreover, the errors due to the virtual space truncation decrease monotonically when the FNO scheme is used. However, the direct application of the FNO strategy to open-shell references, as needed in EOM-SF calculations, leads to much larger errors than in the case of closed-shell references. We analyzed the applicability of the FNO approximation for open-shell CCSD and investigated the reasons for its breakdown in open-shell systems within the EOM-SF-CCSD framework. The main cause of the breakdown is the mismatch between the α and β FNOs and the consequent imbalance between the α and β active orbital spaces. A similar mismatch happens when canonical Hartree–Fock orbitals are frozen, leading to large errors in the computed energies. To address these issues, we developed a new scheme, called OSFNO. Benchmark calculations illustrated that OSFNO delivers robust performance, similarly to the original FNO scheme in the case of closed-shell references. A typical OSFNO population cutoff of 99% leads to the errors in singlet–triplet gaps of 130 cm^{-1} for same-center diradicals, ~10–60 cm^{-1} for benzynes, 20–50 cm^{-1} for dehydro-*meta*-xylylenes, and <18 cm^{-1} for dicopper SMMs. For SMMs, this approach reduces the virtual space by ~22% for cc-pVDZ and by ~46% for cc-pVTZ. Using OSFNO has enabled the EOM-SF-CCSD calculations with more than 1000 basis functions on a single node. Finally, this approximation has a negligible impact on the spin–orbit coupling constants, enabling calculations of magnetic properties in large systems.

SUPPLEMENTARY MATERIAL

See the supplementary material for mean errors and standard deviations, relevant Cartesian coordinates.

ACKNOWLEDGMENTS

This work was supported by the Department of Energy through the DE-SC0018910 grant (A.I.K.). A.I.K. is also a grateful recipient of the Simons Fellowship in Theoretical Physics, which enabled her sabbatical stay in Germany. D.I. is grateful for the support through the summer research program at the Department of Chemistry at USC.

The authors declare the following competing financial interest(s): A.I.K. is a member of the Board of Directors and a part-owner of Q-Chem, Inc.

REFERENCES

[1]T. Helgaker, P. Jørgensen, and J. Olsen, *Molecular Electronic Structure Theory* (Wiley & Sons, 2000).
[2]G. D. Purvis and R. J. Bartlett, "A full coupled-cluster singles and doubles model: The inclusion of disconnected triples," J. Chem. Phys. **76**, 1910 (1982).
[3]J. Noga and R. J. Bartlett, "The full CCSDT model for molecular electronic structure," J. Chem. Phys. **86**, 7041 (1987).
[4]K. Raghavachari, G. W. Trucks, J. A. Pople, and M. Head-Gordon, "A fifth-order perturbation comparison of electron correlation theories," Chem. Phys. Lett. **157**, 479 (1989).
[5]J. D. Watts and R. J. Bartlett, "Economical triple excitation equation-of-motion coupled-cluster methods for excitation-energies," Chem. Phys. Lett. **233**, 81 (1995).
[6]J. D. Watts, J. Gauss, and R. J. Bartlett, "Coupled-cluster methods with noniterative triple excitations for restricted open-shell Hartree-Fock and other general single determinant reference functions. Energies and analytical gradients," J. Chem. Phys. **98**, 8718 (1993).
[7]J. D. Watts and R. J. Bartlett, "Iterative and non-iterative triple excitation corrections in coupled-cluster methods for excited electronic states: The EOM-CCSDT-3 and EOM-CCSD($\tilde{T}$) methods," Chem. Phys. Lett. **258**, 581 (1996).
[8]S. R. Gwaltney and M. Head-Gordon, "A second-order perturbative correction to the coupled-cluster singles and doubles model: CCSD(2)," J. Chem. Phys. **115**, 2014 (2001).
[9]P. U. Manohar and A. I. Krylov, "A non-iterative perturbative triples correction for the spin-flipping and spin-conserving equation-of-motion coupled-cluster methods with single and double substitutions," J. Chem. Phys. **129**, 194105 (2008).
[10]K. Kowalski and P. Piecuch, "New type of noniterative energy corrections for excited electronic states: Extension of the method of moments of coupled-cluster equations to the equation-of-motion coupled-cluster formalism," J. Chem. Phys. **115**, 2966 (2001).
[11]K. Kowalski and P. Piecuch, "New coupled-cluster methods with singles, doubles, and noniterative triples for high accuracy calculations of excited electronic states," J. Chem. Phys. **120**, 1715 (2004).
[12]M. Włoch, M. D. Lodriguito, P. Piecuch, and J. R. Gour, "Two new classes of non-iterative coupled-cluster methods derived from the method of moments of coupled-cluster equations," Mol. Phys. **104**, 2149 (2006).
[13]J. L. Whitten, "Coulombic potential energy integrals and approximations," J. Chem. Phys. **58**, 4496 (1973).
[14]B. I. Dunlap, J. W. D. Connolly, and J. R. Sabin, "On first-row diatomic-molecules and local density models," J. Chem. Phys. **71**, 4993 (1979).
[15]K. Eichkorn, O. Treutler, H. Öhm, M. Häser, and R. Ahlrichs, "Auxiliary basis sets to approximate Coulomb potentials," Chem. Phys. Lett. **240**, 283 (1995).
[16]A. E. DePrince, M. R. Kennedy, B. G. Sumpter, and C. D. Sherrill, "Density-fitted singles and doubles coupled-cluster on graphics processing units," Mol. Phys. **112**, 844 (2014).
[17]D. Kumar, A. K. Dutta, and P. U. Manohar, "Resolution of the identity and Cholesky representation of EOM-MP2 approximation: Implementation, accuracy and efficiency," J. Chem. Sci. **129**, 1611 (2017).
[18]U. Bozkaya and C. D. Sherrill, "Analytic energy gradients for the coupled-cluster singles and doubles method with the density-fitting approximation," J. Chem. Phys. **144**, 174103 (2016).
[19]U. Bozkaya and C. D. Sherrill, "Analytic energy gradients for the coupled-cluster singles and doubles with perturbative triples method with the density-fitting approximation," J. Chem. Phys. **147**, 044104 (2017).
[20]X. Wang, A. Y. Sokolov, J. M. Turney, and H. F. Schaefer, "Spin-adapted formulation and implementation of density cumulant functional theory with

density-fitting approximation: Application to transition metal compounds," J. Chem. Theory Comput. **12**, 4833 (2016).
[21]T. Shen, Z. Zhu, I. Y. Zhang, and M. Scheffler, "Massive-parallel implementation of the resolution-of-identity coupled-cluster approaches in the numeric atom-centered orbital framework for molecular systems," J. Chem. Theory Comput. **15**, 4721 (2019).
[22]N. H. F. Beebe and J. Linderberg, "Simplifications in the generation and transformation of two-electron integrals in molecular calculations," Int. J. Quant. Chem. **12**, 683 (1977).
[23]H. Koch, A. S. de Merás, and T. B. Pedersen, "Reduced scaling in electronic structure calculations using Cholesky decompositions," J. Chem. Phys. **118**, 9481 (2003).
[24]F. Aquilante, R. Lindh, and T. B. Pedersen, "Unbiased auxiliary basis sets for accurate two-electron integral approximations," J. Chem. Phys. **127**, 114107 (2007).
[25]L. Boman, H. Koch, and A. Sanchez de Meras, "Method specific Cholesky decomposition: Coulomb and exchange energies," J. Chem. Phys. **129**, 134107 (2008).
[26]F. Aquilante, T. B. Pedersen, and R. Lindh, "Density fitting with auxiliary basis sets from Cholesky decompositions," Theor. Chem. Acc. **124**, 1 (2009).
[27]F. Aquilante, L. Gagliardi, T. B. Pedersen, and R. Lindh, "Atomic Cholesky decompositions: A route to unbiased auxiliary basis sets for density fitting approximation with tunable accuracy and efficiency," J. Chem. Phys. **130**, 154107 (2009).
[28]F. Aquilante, L. Boman, J. Boström, H. Koch, R. Lindh, A. S. de Merás, and T. B. Pedersen, "Cholesky decomposition techniques in electronic structure theory," in *Linear-Scaling Techniques in Computational Chemistry and Physics*, Challenges and advances in computational chemistry and physics, edited by R. Zaleśny, M. G. Papadopoulos, P. G. Mezey, and J. Leszczynski (Springer, 2011), pp. 301–343.
[29]E. Epifanovsky, D. Zuev, X. Feng, K. Khistyaev, Y. Shao, and A. I. Krylov, "General implementation of resolution-of-identity and Cholesky representations of electron-repulsion integrals within coupled-cluster and equation-of-motion methods: Theory and benchmarks," J. Chem. Phys. **139**, 134105 (2013).
[30]S. D. Folkestad, E. F. Kjønstad, and H. Koch, "An efficient algorithm for Cholesky decomposition of electron repulsion integrals," J. Chem. Phys. **150**, 194112 (2019).
[31]X. Feng, E. Epifanovsky, J. Gauss, and A. I. Krylov, "Implementation of analytic gradients for CCSD and EOM-CCSD using Cholesky decomposition of the electron-repulsion integrals and their derivatives: Theory and benchmarks," J. Chem. Phys. **151**, 014110 (2019).
[32]T. J. Martínez, A. Mehta, and E. A. Carter, "Pseudospectral full configuration interaction," J. Chem. Phys. **97**, 1876 (1992).
[33]T. J. Martínez and E. A. Carter, "Pseudospectral Møller–Plesset perturbation theory through third order," J. Chem. Phys. **100**, 3631 (1994).
[34]T. J. Martínez and E. A. Carter, "Pseudospectral multireference single and double excitation configuration interaction," J. Chem. Phys. **102**, 7564 (1995).
[35]S. Kossmann and F. Neese, "Efficient structure optimization with second-order many-body perturbation theory: The RIJCOSX-MP2 method," J. Chem. Theory Comput. **6**, 2325 (2010).
[36]F. Neese, F. Wennmohs, A. Hansen, and U. Becker, "Efficient, approximate and parallel Hartree–Fock and hybrid DFT calculations. A 'chain-of-spheres' algorithm for the Hartree–Fock exchange," Chem. Phys. **356**, 98 (2009).
[37]A. K. Dutta, F. Neese, and R. Izsák, "Speeding up equation of motion coupled cluster theory with the chain of spheres approximation," J. Chem. Phys. **144**, 034102 (2016).
[38]E. G. Hohenstein, R. M. Parrish, and T. J. Martínez, "Tensor hypercontraction density fitting. I. Quartic scaling second- and third-order Møller-Plesset perturbation theory," J. Chem. Phys. **137**, 044103 (2012).
[39]E. G. Hohenstein, R. M. Parrish, C. D. Sherrill, and T. J. Martínez, "Communication: Tensor hypercontraction. III. Least-squares tensor hypercontraction for the determination of correlated wavefunctions," J. Chem. Phys. **137**, 221101 (2012).
[40]R. M. Parrish, E. G. Hohenstein, T. J. Martínez, and C. D. Sherrill, "Tensor hypercontraction. II. Least-squares renormalization," J. Chem. Phys. **137**, 224106 (2012).
[41]S. I. L. Kokkila Schumacher, E. G. Hohenstein, R. M. Parrish, L.-P. Wang, and T. J. Martínez, "Tensor hypercontraction second-order Møller–Plesset perturbation theory: Grid optimization and reaction energies," J. Chem. Theory Comput. **11**, 3042 (2015).
[42]E. G. Hohenstein, S. I. L. Kokkila, R. M. Parrish, and T. J. Martínez, "Tensor hypercontraction equation-of-motion second-order approximate coupled cluster: Electronic excitation energies in $O(N^4)$ time," J. Phys. Chem. B **117**, 12972 (2013).
[43]J. Brabec, C. Yang, E. Epifanovsky, A. I. Krylov, and E. Ng, "Reduced-cost sparcity-exploiting algorithm for solving coupled-cluster equations," J. Comput. Chem. **37**, 1059 (2016).
[44]R. M. Parrish, Y. Zhao, E. G. Hohenstein, and T. J. Martínez, "Rank reduced coupled cluster theory. I. Ground state energies and wavefunctions," J. Chem. Phys. **150**, 164118 (2019).
[45]N. K. Madsen, I. H. Godtliebsen, S. A. Losilla, and O. Christiansen, "Tensor-decomposed vibrational coupled-cluster theory: Enabling large-scale, highly accurate vibrational-structure calculations," J. Chem. Phys. **148**, 024103 (2018).
[46]N. J. Mayhall, "Using higher-order singular value decomposition to define weakly coupled and strongly correlated clusters: The n-body Tucker approximation," J. Chem. Theory Comput. **13**, 4818 (2017).
[47]P. Pulay, "Localizability of dynamic electron correlation," Chem. Phys. Lett. **100**, 151 (1983).
[48]P. Pulay and S. Saebø, "Orbital-invariant formulation and second-order gradient evaluation in Møller-Plesset perturbation-theory," Theor. Chim. Acta **69**, 357 (1986).
[49]S. Saebø and P. Pulay, "Fourth-order Møller-Plesset perturbation theory in the local correlation treatment. I. Method," J. Chem. Phys. **86**, 914 (1987).
[50]S. Saebø and P. Pulay, "Local configuration interaction: An efficient approach for larger molecules," Chem. Phys. Lett. **113**, 13 (1985).
[51]M. Schütz, G. Hetzer, and H.-J. Werner, "Low-order scaling local electron correlation methods. I. Linear scaling local MP2," J. Chem. Phys. **111**, 5691 (1999).
[52]G. Hetzer, M. Schütz, H. Stoll, and H.-J. Werner, "Low-order scaling local correlation methods II: Splitting the Coulomb operator in linear scaling local second-order Møller-Plesset perturbation theory," J. Chem. Phys. **113**, 9443 (2000).
[53]H.-J. Werner and M. Schütz, "An efficient local coupled cluster method for accurate thermochemistry of large systems," J. Chem. Phys. **135**, 144116 (2011).
[54]M. Schütz and H.-J. Werner, "Low-order scaling local electron correlation methods. IV. Linear scaling local coupled-cluster (LCCSD)," J. Chem. Phys. **114**, 661 (2001).
[55]M. Schütz and H.-J. Werner, "Local perturbative triples correction (T) with linear cost scaling," Chem. Phys. Lett. **318**, 370 (2000).
[56]M. Schütz, "Low-order scaling local electron correlation methods. III. Linear scaling local perturbative triples correction (T)," J. Chem. Phys. **113**, 9986 (2000).
[57]M. Schütz, O. Masur, and D. Usvyat, "Efficient and accurate treatment of weak pairs in local CCSD(t) calculations. II. Beyond the ring approximation," J. Chem. Phys. **140**, 244107 (2014).
[58]M. Schütz, "Low-order scaling local electron correlation methods. V. Connected triples beyond (T): Linear scaling local CCSDT-1b," J. Chem. Phys. **116**, 8772 (2002).
[59]P.-O. Löwdin, "Quantum theory of many-particle systems. I. Physical interpretations by means of density matrices, natural spin-orbitals, and convergence problems in the method of configurational interaction," Phys. Rev. **97**, 1474 (1955).
[60]C. F. Bender and E. R. Davidson, "Theoretical calculation of the potential curves of the Be_2 molecule," J. Chem. Phys. **47**, 4972 (1967).
[61]R. J. Buenker and S. D. Peyerimhoff, "Individualized configuration selection in CI calculations with subsequent energy extrapolation," Theor. Chim. Acta **35**, 33 (1974).
[62]K. H. Thunemann, J. Römelt, S. D. Peyerimhoff, and R. J. Buenker, "A study of the convergence in iterative natural orbital procedures," Int. J. Quant. Chem. **11**, 743 (1977).
[63]R. J. Cave, S. S. Xantheas, and D. Feller, "Exploiting regularity in systematic sequences of wave-functions which approach the full CI limit," Theor. Chim. Acta **83**, 31 (1992).

[64]C. D. Sherrill and H. F. Schaefer III, "The configuration interaction method: Advances in highly correlated approaches," Adv. Quantum Chem. **34**, 143 (1999).
[65]J. Ivanic and K. Ruedenberg, "Deadwood in configuration spaces. II. Singles plus doubles and singles plus doubles plus triples plus quadruples spaces," Theor. Chim. Acta **107**, 220 (2002).
[66]M. L. Abrams and C. D. Sherrill, "A comparison of polarized double-zeta basis sets and natural orbitals for full configuration interaction benchmarks," J. Chem. Phys. **118**, 1604 (2003).
[67]Z. Lu and S. Matsika, "High-multiplicity natural orbitals in multireference configuration interaction for excited states," J. Chem. Theory Comput. **8**, 509 (2011).
[68]Z. Lu and S. Matsika, "High-multiplicity natural orbitals in multireference configuration interaction for excited state potential energy surfaces," J. Phys. Chem. A **117**, 7421 (2013).
[69]F. Neese, F. Wennmohs, and A. Hansen, "Efficient and accurate local approximations to coupled-electron pair approaches: An attempt to revive the pair natural orbital method," J. Chem. Phys. **130**, 114108 (2009).
[70]P. R. Nagy, G. Samu, and M. Kállay, "Optimization of the linear-scaling local natural orbital CCSD(T) method: Improved algorithm and benchmark applications," J. Chem. Theory Comput. **14**, 4193 (2018).
[71]C. Riplinger and F. Neese, "An efficient and near linear scaling pair natural orbital based local coupled cluster method," J. Chem. Phys. **138**, 034106 (2013).
[72]F. Neese, A. Hansen, and D. G. Liakos, "Efficient and accurate approximations to the local coupled cluster singles doubles method using a truncated pair natural orbital basis," J. Chem. Phys. **131**, 064103 (2009).
[73]C. Riplinger, B. Sandhoefer, A. Hansen, and F. Neese, "Natural triple excitations in local coupled cluster calculations with pair natural orbitals," J. Chem. Phys. **139**, 134101 (2013).
[74]P. Pinski, C. Riplinger, E. F. Valeev, and F. Neese, "Sparse maps—A systematic infrastructure for reduced-scaling electronic structure methods. I. An efficient and simple linear scaling local MP2 method that uses an intermediate basis of pair natural orbitals," J. Chem. Phys. **143**, 034108 (2015).
[75]C. Riplinger, P. Pinski, U. Becker, E. F. Valeev, and F. Neese, "Sparse maps—A systematic infrastructure for reduced-scaling electronic structure methods. II. Linear scaling domain based pair natural orbital coupled cluster theory," J. Chem. Phys. **144**, 024109 (2016).
[76]M. Saitow, U. Becker, C. Riplinger, E. F. Valeev, and F. Neese, "A new near-linear scaling, efficient and accurate, open-shell domain-based local pair natural orbital coupled cluster singles and doubles theory," J. Chem. Phys. **146**, 164105 (2017).
[77]A. K. Dutta, M. Saitow, C. Riplinger, F. Neese, and R. Izsák, "A near-linear scaling equation of motion coupled cluster method for ionized states," J. Chem. Phys. **148**, 244101 (2018).
[78]T. L. Barr and E. R. Davidson, "Nature of the configuration-interaction method in *ab initio* calculations. I. Ne ground state," Phys. Rev. A **1**, 644 (1970).
[79]C. Sosa, J. Geertsen, G. W. Trucks, and R. J. Bartlett, "Selection of the reduced virtual space for correlated calculations. An application to the energy and dipole-moment of H_2O," Chem. Phys. Lett. **159**, 148 (1989).
[80]A. G. Taube and R. J. Bartlett, "Frozen natural orbitals: Systematic basis set truncation for coupled-cluster theory," Collect. Czech. Chem. Commun. **70**, 837 (2005).
[81]A. G. Taube and R. J. Bartlett, "Frozen natural orbital coupled-cluster theory: Forces and application to decomposition of nitroethane," J. Chem. Phys. **128**, 164101 (2008).
[82]A. E. DePrince and C. D. Sherrill, "Accurate noncovalent interaction energies using truncated basis sets based on frozen natural orbitals," J. Chem. Theory Comput. **9**, 293 (2013).
[83]A. Kumar and T. D. Crawford, "Frozen virtual natural orbitals for coupled-cluster linear-response theory," J. Phys. Chem. A **121**, 708 (2017).
[84]T. D. Crawford, A. Kumar, A. P. Bazanté, and R. Di Remigio, "Reduced-scaling coupled cluster response theory: Challenges and opportunities," Wiley Interdiscip. Rev.: Comput. Mol. Sci. **9**, e1406 (2019).
[85]D. Mester, P. R. Nagy, and M. Kállay, "Reduced-cost linear-response CC2 method based on natural orbitals and natural auxiliary functions," J. Chem. Phys. **146**, 194102 (2017).
[86]C. Peng, M. C. Clement, and E. F. Valeev, "State-averaged pair natural orbitals for excited states: A route toward efficient equation of motion coupled-cluster," J. Chem. Theory Comput. **14**, 5597 (2018).
[87]S. Höfener and W. Klopper, "Natural transition orbitals for the calculation of correlation and excitation energies," Chem. Phys. Lett. **679**, 52 (2017).
[88]P. Baudin and K. Kristensen, "Correlated natural transition orbital framework for low-scaling excitation energy calculations (CorNFLEx)," J. Chem. Phys. **146**, 214114 (2017).
[89]A. I. Krylov, "Equation-of-motion coupled-cluster methods for open-shell and electronically excited species: The hitchhiker's guide to Fock space," Annu. Rev. Phys. Chem. **59**, 433 (2008).
[90]R. J. Bartlett, "The coupled-cluster revolution," Mol. Phys. **108**, 2905 (2010).
[91]K. Sneskov and O. Christiansen, "Excited state coupled cluster methods," Wiley Interdiscip. Rev.: Comput. Mol. Sci. **2**, 566 (2012).
[92]R. J. Bartlett, "Coupled-cluster theory and its equation-of-motion extensions," Wiley Interdiscip. Rev.: Comput. Mol. Sci. **2**, 126 (2012).
[93]A. Landau, K. Khistyaev, S. Dolgikh, and A. I. Krylov, "Frozen natural orbitals for ionized states within equation-of-motion coupled-cluster formalism," J. Chem. Phys. **132**, 014109 (2010).
[94]J. F. Stanton and J. Gauss, "Analytic energy derivatives for ionized states described by the equation-of-motion coupled cluster method," J. Chem. Phys. **101**, 8938 (1994).
[95]P. A. Pieniazek, S. E. Bradforth, and A. I. Krylov, "Charge localization and Jahn-Teller distortions in the benzene dimer cation," J. Chem. Phys. **129**, 074104 (2008).
[96]M. Nooijen and R. J. Bartlett, "Equation of motion coupled cluster method for electron attachment," J. Chem. Phys. **102**, 3629 (1995).
[97]A. I. Krylov, "Size-consistent wave functions for bond-breaking: The equation-of-motion spin-flip model," Chem. Phys. Lett. **338**, 375 (2001).
[98]D. Casanova, L. V. Slipchenko, A. I. Krylov, and M. Head-Gordon, "Double spin-flip approach within equation-of-motion coupled cluster and configuration interaction formalisms: Theory, implementation and examples," J. Chem. Phys. **130**, 044103 (2009).
[99]A. I. Krylov, "The spin-flip equation-of-motion coupled-cluster electronic structure method for a description of excited states, bond-breaking, diradicals, and triradicals," Acc. Chem. Res. **39**, 83 (2006).
[100]F. Aquilante, T. K. Todorova, L. Gagliardi, T. B. Pedersen, and B. O. Roos, "Systematic truncation of the virtual space in multiconfigurational perturbation theory," J. Chem. Phys. **131**, 034113 (2009).
[101]J. Segarra-Martí, M. Garavelli, and F. Aquilante, "Multiconfigurational second-order perturbation theory with frozen natural orbitals extended to the treatment of photochemical problems," J. Chem. Theory Comput. **11**, 3772 (2015).
[102]J. F. Stanton and R. J. Bartlett, "The equation of motion coupled-cluster method. A systematic biorthogonal approach to molecular excitation energies, transition probabilities, and excited state properties," J. Chem. Phys. **98**, 7029 (1993).
[103]A. Tajti and P. G. Szalay, "Analytic evaluation of the nonadiabatic coupling vector between excited states using equation-of-motion coupled-cluster theory," J. Chem. Phys. **131**, 124104 (2009).
[104]S. Faraji, S. Matsika, and A. I. Krylov, "Calculations of non-adiabatic couplings within equation-of-motion coupled-cluster framework: Theory, implementation, and validation against multi-reference methods," J. Chem. Phys. **148**, 044103 (2018).
[105]P. Pokhilko, E. Epifanovsky, and A. I. Krylov, "General framework for calculating spin–orbit couplings using spinless one-particle density matrices: Theory and application to the equation-of-motion coupled-cluster wave functions," J. Chem. Phys. **151**, 034106 (2019).
[106]L. V. Slipchenko and A. I. Krylov, "Singlet-triplet gaps in diradicals by the spin-flip approach: A benchmark study," J. Chem. Phys. **117**, 4694 (2002).
[107]N. Orms and A. I. Krylov, "Singlet-triplet energy gaps and the degree of diradical character in binuclear copper molecular magnets characterized by spin-flip density functional theory," Phys. Chem. Chem. Phys. **20**, 13127 (2018).
[108]N. J. Mayhall and M. Head-Gordon, "Computational quantum chemistry for multiple-site Heisenberg spin couplings made simple: Still only one spin-flip required," J. Phys. Chem. Lett. **6**, 1982 (2015).

[109]Y. Shao, Z. Gan, E. Epifanovsky, A. T. B. Gilbert, M. Wormit, J. Kussmann, A. W. Lange, A. Behn, J. Deng, X. Feng, D. Ghosh, M. Goldey, P. R. Horn, L. D. Jacobson, I. Kaliman, R. Z. Khaliullin, T. Kus, A. Landau, J. Liu, E. I. Proynov, Y. M. Rhee, R. M. Richard, M. A. Rohrdanz, R. P. Steele, E. J. Sundstrom, H. L. Woodcock III, P. M. Zimmerman, D. Zuev, B. Albrecht, E. Alguires, B. Austin, G. J. O. Beran, Y. A. Bernard, E. Berquist, K. Brandhorst, K. B. Bravaya, S. T. Brown, D. Casanova, C.-M. Chang, Y. Chen, S. H. Chien, K. D. Closser, D. L. Crittenden, M. Diedenhofen, R. A. DiStasio, Jr., H. Do, A. D. Dutoi, R. G. Edgar, S. Fatehi, L. Fusti-Molnar, A. Ghysels, A. Golubeva-Zadorozhnaya, J. Gomes, M. W. D. Hanson-Heine, P. H. P. Harbach, A. W. Hauser, E. G. Hohenstein, Z. C. Holden, T.-C. Jagau, H. Ji, B. Kaduk, K. Khistyaev, J. Kim, J. Kim, R. A. King, P. Klunzinger, D. Kosenkov, T. Kowalczyk, C. M. Krauter, K. U. Laog, A. Laurent, K. V. Lawler, S. V. Levchenko, C. Y. Lin, F. Liu, E. Livshits, R. C. Lochan, A. Luenser, P. Manohar, S. F. Manzer, S.-P. Mao, N. Mardirossian, A. V. Marenich, S. A. Maurer, N. J. Mayhall, C. M. Oana, R. Olivares-Amaya, D. P. O'Neill, J. A. Parkhill, T. M. Perrine, R. Peverati, P. A. Pieniazek, A. Prociuk, D. R. Rehn, E. Rosta, N. J. Russ, N. Sergueev, S. M. Sharada, S. Sharmaa, D. W. Small, A. Sodt, T. Stein, D. Stuck, Y.-C. Su, A. J. W. Thom, T. Tsuchimochi, L. Vogt, O. Vydrov, T. Wang, M. A. Watson, J. Wenzel, A. White, C. F. Williams, V. Vanovschi, S. Yeganeh, S. R. Yost, Z.-Q. You, I. Y. Zhang, X. Zhang, Y. Zhou, B. R. Brooks, G. K. L. Chan, D. M. Chipman, C. J. Cramer, W. A. Goddard III, M. S. Gordon, W. J. Hehre, A. Klamt, H. F. Schaefer III, M. W. Schmidt, C. D. Sherrill, D. G. Truhlar, A. Warshel, X. Xu, A. Aspuru-Guzik, R. Baer, A. T. Bell, N. A. Besley, J.-D. Chai, A. Dreuw, B. D. Dunietz, T. R. Furlani, S. R. Gwaltney, C.-P. Hsu, Y. Jung, J. Kong, D. S. Lambrecht, W. Z. Liang, C. Ochsenfeld, V. A. Rassolov, L. V. Slipchenko, J. E. Subotnik, T. Van Voorhis, J. M. Herbert, A. I. Krylov, P. M. W. Gill, and M. Head-Gordon, "Advances in molecular quantum chemistry contained in the Q-Chem 4 program package," Mol. Phys. **113**, 184 (2015).

[110]A. I. Krylov and P. M. W. Gill, "Q-Chem: An engine for innovation," Wiley Interdiscip. Rev.: Comput. Mol. Sci. **3**, 317 (2013).

[111]Y. A. Bernard, Y. Shao, and A. I. Krylov, "General formulation of spin-flip time-dependent density functional theory using non-collinear kernels: Theory, implementation, and benchmarks," J. Chem. Phys. **136**, 204103 (2012).

[112]P. Pokhilko, E. Epifanovskii, and A. I. Krylov, "Double precision is not needed for many-body calculations: Emergent conventional wisdom," J. Chem. Theory Comput. **14**, 4088 (2018).

[113]R. S. Mulliken, "Report on notation for the spectra of polyatomic molecules," J. Chem. Phys. **23**, 1997 (1955).

[114]Depending on molecular orientation, symmetry labels corresponding to the same orbital or vibrational mode may be different. Q-Chem's standard molecular orientation is different from that of Mulliken.[113] For example, Q-Chem places water molecule in the *xz*-plane instead of *yz*. Consequently, for C_{2v} symmetry, b_1 and b_2 labels are flipped. More details can be found at http://iopenshell.usc.edu/resources/howto/symmetry.

[115]A. I. Krylov, "Triradicals," J. Phys. Chem. A **109**, 10638 (2005).

[116]N. Orms, D. R. Rehn, A. Dreuw, and A. I. Krylov, "Characterizing bonding patterns in diradicals and triradicals by density-based wave function analysis: A uniform approach," J. Chem. Theory Comput. **14**, 638 (2017).

[117]T. Wang and A. I. Krylov, "Electronic structure of the two dehydro-meta-xylylene triradicals and their derivatives," Chem. Phys. Lett. **425**, 196 (2006).

[118]T. Wang and A. I. Krylov, "The effect of substituents on singlet-triplet energy separations in meta-xylylene diradicals: Qualitative insights from quantitative studies," J. Chem. Phys. **123**, 104304 (2005).

[119]L. V. Slipchenko and A. I. Krylov, "Electronic structure of the 1,3,5,-tridehydrobenzene triradical in its ground and excited states," J. Chem. Phys. **118**, 9614 (2003).

[120]A. M. C. Cristian, Y. Shao, and A. I. Krylov, "Bonding patterns in benzene triradicals from structural, spectroscopic, and thermochemical perspectives," J. Phys. Chem. A **108**, 6581 (2004).

[121]P. U. Manohar, L. Koziol, and A. I. Krylov, "Effect of a heteroatom on bonding patterns and triradical stabilization energies of 2,4,6-tridehydropyridine versus 1,3,5-tridehydrobenzene," J. Phys. Chem. A **113**, 2519 (2009).

[122]The effect of orbital optimization on spin contamination was studied, for example, in Ref. 130.

[123]C. D. Sherrill, A. I. Krylov, E. F. C. Byrd, and M. Head-Gordon, "Energies and analytic gradients for a coupled-cluster doubles model using variational Brueckner orbitals: Application to symmetry breaking in O_4^+," J. Chem. Phys. **109**, 4171 (1998).

[124]J. Lee and M. Head-Gordon, "Regularized orbital-optimized second-order Møller–Plesset perturbation theory: A reliable fifth-order-scaling electron correlation model with orbital energy dependent regularizers," J. Chem. Theory Comput. **14**, 5203 (2018).

[125]J. Lee and M. Head-Gordon, "Distinguishing artificial and essential symmetry breaking in a single determinant: Approach and application to the C_{60}, C_{36}, and C_{20} fullerenes," Phys. Chem. Chem. Phys. **21**, 4763 (2019).

[126]P. G. Wenthold, "Spin-state dependent radical stabilization in nitrenes: The unusually small singlet–triplet splitting in 2-furanylnitrene," J. Org. Chem. **77**, 208 (2012).

[127]E. Hossain and P. G. Wenthold, "Singlet stabilization of oxazole-and isoxazolenitrene-n-oxides by radical delocalization," Comput. Theor. Chem. **1020**, 180 (2013).

[128]E. Hossain, S. M. Deng, S. Gozem, A. I. Krylov, X.-B. Wang, and P. G. Wenthold, "Photoelectron spectroscopy study of quinonimides," J. Am. Chem. Soc. **139**, 11138 (2017).

[129]L. V. Slipchenko, T. E. Munsch, P. G. Wenthold, and A. I. Krylov, "5-dehydro-1,3-quinodimethane: A hydrocarbon with an open-shell doublet ground state," Angew. Chem., Int. Ed. **43**, 742 (2004).

[130]A. I. Krylov, "Spin-contamination in coupled cluster wavefunctions," J. Chem. Phys. **113**, 6052 (2000).